Homopolymer Distributions in Ordered Block Copolymers

A. M. Mayes and T. P. Russell*

IBM Research Division, Almaden Research Center, 650 Harry Road, San Jose, California 95120-6099

S. K. Satija and C. F. Majkrzak

Reactor Radiation Division, National Institute of Standards and Technology, Gaithersburg, Maryland 20899

Received April 6, 1992; Revised Manuscript Received July 23, 1992

ABSTRACT: Mixtures of polystyrene (PS) or poly(methyl methacrylate) (PMMA) homopolymers with symmetric P(S-*b*-MMA) diblock copolymers were investigated by neutron reflectivity. In a thin-film geometry, these mixtures form alternating lamellar microdomains oriented parallel to the substrate surface. By adding perdeuterated homopolymer to unlabeled copolymer, the spatial distribution of the homopolymer was characterized quantitatively. When the molecular weight of the homopolymer is comparable to the block molecular weight, the homopolymer is confined to the corresponding copolymer domain, with a distribution which peaks at the center of the domain. The results are shown to be in excellent agreement with mean-field predictions. With decreasing molecular weight, the homopolymer is more uniformly distributed within the domain. When the molecular weight of the homopolymer is much larger than the block molecular weight, the homopolymer is excluded from the lamellar microdomains, but does not interfere with the preferred lamellar orientation and is incorporated into the multilayered morphology.

I. Introduction

In block copolymer melts incompatibility between unlike segments results in the formation of ordered microdomains that exhibit periodicity on the length scale of the copolymer radius of gyration. The equilibrium microdomain morphology is a strong function of the copolymer composition. When the volume fractions of the two copolymer components are comparable, alternating lamellar domains are formed. As the copolymer composition is made increasingly asymmetric, curvature is induced in the system such that bicontinuous double-diamond nets, hexagonal-packed cylinder arrays, and body-centered cubic packed spheres are observed, in turn, as equilibrium morphologies.[1-3] Analogously, the addition of a homopolymer which segregates preferentially to one block domain can introduce curvature and drive a change in morphology.[4]

While numerous theoretical and experimental articles have been published on the thermodynamics of pure block copolymer systems, the rich phase diagrams for block copolymer/homopolymer blends are less well characterized.[4,5] Several groups have examined the effects of moderate additions (<30%) of polystyrene homopolymers on the morphology of nearly symmetric poly(styrene-*b*-isoprene) diblock copolymers using transmission electron microscopy and small-angle scattering.[6-8] An early investigation by Ptaszynski et al.[6] and more recent studies[7-9] suggest that when the homopolystyrene molecular weight is below or comparable to that of the PS block, the homopolymer is completely solubilized in the PS lamellar domains. The lamellar spacing and PS domain size are generally observed to increase with increasing homopolymer content, while the PI domain width decreases to maintain constant density. Winey et al.[8] found a decrease in lamellar spacing relative to the pure copolymer in blends with low molecular weight PS homopolymer. For a fixed blend concentration, Hashimoto et al.[7] and Winey et al.[8] determined that the PS domains expand less for lower molecular weight homopolymer, while the PI domains contract more. These trends suggest that lower molecular weight polystyrene homopolymer is more uniformly distributed through the PS microdomains, while higher molecular weight homopolymer is more centralized, or sandwiched, between PS blocks of the copolymer. The solubility of homopolymer in the ordered domains decreases with increasing molecular weight. Ptaszynski et al.[6] found that blends containing 20% polystyrene with molecular weights over twice that of the PS copolymer block turned opaque, indicating macroscopic phase separation. From the calculated lamellar spacing for these samples, the homopolymer was determined to be partially miscible in the PS domains. A later study by Quan et al.[10] found decreasing miscibility of polybutadiene homopolymers in ordered poly(styrene–butadiene–styrene) triblock copolymers as the homopolymer molecular weight increased beyond half that of the polybutadiene block.

While prior studies lend much insight into the morphological behavior of blends of symmetric copolymers with homopolymers of varying molecular weight, the distribution of the homopolymer chains within the copolymer domains has only been discussed qualitatively.[7,8] In the present study, neutron reflectivity is used to obtain quantitative information on the distribution of polystyrene (PS) or poly(methyl methacrylate) (PMMA) homopolymers in ordered films of symmetric P(S-*b*-MMA) diblock copolymers. In thin block copolymer films, preferential interactions of the copolymer blocks with the substrate and air interfaces result in near-perfect orientation of the lamellar domains parallel to the surface. Such films provide model systems to analyze ordered copolymers by neutron reflectivity. In earlier studies, the selective deuteration of one copolymer block has provided detailed information on domain sizes and interfacial widths in well-ordered P(S-*b*-MMA) diblock films.[11,12] With the addition of a homopolymer labeled to match the corresponding copolymer block, such as PMMA homopolymer blended with P(d-S-*b*-MMA) copolymer, changes in the lamellar spacing and domain sizes as a function of homopolymer concentration and molecular weight are readily obtained. The addition of deuterium-labeled homopolymers to an unlabeled copolymer reveals homopolymer distributions within the copolymer microdomains. The results are compared with distributions predicted by a recent mean-

* To whom correspondence should be addressed.

0024-9297/92/2225-6523$03.00/0

Table I
Characteristics of Copolymers and Mixtures with Homopolymers

sample	description[a,b]	vol % of PMMA calcd	vol % of PMMA measd	$\varphi_h \times 100$ calcd	$\varphi_h \times 100$ measd
HH0[c]	P(S-*b*-MMA) 91K		53		
HH1	+5% d-PMMA 57K	53[d]	53	4.5	5.0
HH2	+5% d-PMMA 57K +5% PS 52K	52	52	4.5	4.6
HH3	+10% d-PMMA 57K	55[d]	55	9.0	9.4
HH4	+10% d-PMMA 12K	57	57	9.0	8.1
HH5	+5% d-PS 50K	48[d]	48	4.8	4.2
HH6	+10% d-PS 50K	46[d]	47	9.7	7.7
HH7	+5% d-PS 500K	50	53	4.8	5.3
HH8	+10% d-PS 500K	48	54	9.7	10.3
DH0[e]	P(d-S-*b*-MMA) 101K		48		
DH1	+5% PMMA 64K	51	51	5.0	
DH2	+10% PMMA 64K	53	54	9.9	
DH3	+10% PMMA 9.2K	53	54	9.9	
DH4	+5% d-PS 50K	46	46	5.0	
DH5	+10% d-PS 50K	43	44	10.0	
DH6	+5% d-PS 500K	46	48	5.0	
DH7	+10% d-PS 500K	43	48	10.0	

[a] The designation of K indicates the molecular weight in thousands. PS and PMMA denote polystyrene and poly(methyl methacrylate) homopolymers. Perdeuteration is denoted with the prefix d. [b] All percentages noted in this column are weight percentages. [c] The total molecular weight of P(S-*b*-MMA), HH0, is 9.1×10^4 ($M_w/M_n = 1.05$) with a PS block weight-average molecular weight of 4.2×10^4. The number of PS segments, N_{PS}, is 400 and of PMMA segments, N_{PMMA}, is 500, yielding a PS volume fraction, f_S, of 0.47. This copolymer contains ~7% triblock impurity. [d] Values were calculated assuming a 4% by volume impurity of PS homopolymer in the diblock copolymer. These blends were prepared prior to copolymer purification. [e] The total molecular weight of P(d-S-*b*-MMA), DH0, is 10.1×10^4 ($M_w/M_n = 1.04$) with a PS block weight-average molecular weight of 5.3×10^4. $N_{PS} = 470$, $N_{PMMA} = 480$, and $f_S = 0.52$. This copolymer contains ~4% triblock impurity.

field analysis for homopolymers present in lamellar domains of strongly segregated block copolymers.

The current work does not attempt an exhaustive study of copolymer/homopolymer blends in thin-film geometries. Rather, the thin-film morphologies of symmetric diblock copolymers blended with homopolymers having molecular weights lower than, equal to, or higher than the corresponding block molecular weight are compared with the morphologies previously observed in bulk systems.[6-8] A quantitative analysis of homopolymer distributions in ordered copolymer microdomains is presented.

II. Experimental Section

Polished silicon substrates 10 cm in diameter and 4.8 mm thick with the (100) planes oriented parallel to the surface were purchased from Semiconductor Processing Co. Substrates were placed in chromic acid overnight, thoroughly rinsed with deionized water, and allowed to air-dry. Prior to use, substrates were immersed in sulfuric acid approximately 5 min, thoroughly rinsed with deionized water, placed in a 2-propanol vapor degreasing chamber for 5 min, and dried at 110 °C.

Anionically synthesized PS and PMMA homopolymers and P(S-*b*-MMA) diblock copolymers were purchased from Polymer Laboratories. Prior to use, PS homopolymer impurities generated in the diblock synthesis were removed by Soxhlet extraction with cyclohexane. Small amounts of triblock, a product of coupling reactions in the synthesis, were not removed from the copolymers but are expected to have little influence on the blend morphologies at the temperatures of interest. Molecular weight and composition characteristics of the copolymers and blends examined in this study are provided in Table I. Both copolymers were approximately 10^5 in molecular weight, while homopolymer molecular weights ranged between 10^4 and 5×10^5.

Thin films of homopolymer/copolymer mixtures containing 5 or 10 wt % homopolymer were prepared by spin casting from toluene solutions of approximately 3% (w/v). Samples were cast onto silicon substrates at 2000 rpm to obtain thicknesses between 1300 and 1600 Å (corresponding approximately to 3.5 lamellar periods). Specimens were subsequently annealed under vacuum at 160 °C for 5–10 days to achieve ordering. Ellipsometry was used to determine film thicknesses prior to annealing.

Neutron reflectivity measurements were performed on the BT-7 instrument at the National Institute of Standards and Technology. The experimental setup and sample alignment procedure have been described in detail elsewhere.[12] A collimated neutron beam from the reactor is passed through a graphite monochromator delivering neutrons having a wavelength, λ, of 2.37 Å. Following the monochromator, the beam is collimated by two pairs of lithiated polyethylene slits separated by 1.5 m, one near the monochromator, the other near the sample. This produces $\Delta\lambda/\lambda \simeq 0.01$. To gain intensity at higher angles, the slit nearer the specimen is opened stepwise with increasing incidence angle, θ. The angular divergence of the beam varies from 0.017° at the lowest angles to ~0.03° at $\theta = 1.5°$. Beyond the sample a second pair of lithiated polyethylene slits serves to limit background intensity.

Reflectivity curves were generated by rotating the sample θ and the detector 2θ degrees with reference to the incident beam. Data points were taken in steps of 0.01° in θ up to angles >1.5° or 0.07 Å^{-1} in neutron momentum, $k_{z,0} = (2\pi/\lambda)\sin\theta$. Typically, 8 h was required for each reflectivity measurement. Background intensities were obtained by offsetting 2θ by +0.25°. Background was taken in 0.05° steps in θ and extrapolated linearly between points. After background subtraction the net intensity was divided by the main beam intensity with the appropriate slit configurations to produce the reflectivity profiles.

III. Model Reflectivity Profiles

In specular reflectivity, radiation incident on a surface at a glancing angle θ is detected at a corresponding angle θ from the surface after undergoing reflection, thereby recording the momentum transfer normal to the surface. For neutron reflectivity the number of neutrons reflected at an interface between two media depends upon the neutron refractive index of each medium. The neutron momentum normal to the surface, i.e., in the z-direction, in medium j is written as[13]

$$k_{z,j} = [k_{z,0}^2 - 4\pi(b/V)_j]^{1/2} \tag{1}$$

where $(b/V)_j$ is the scattering length density of the medium and $k_{z,0}$ is the z-component of the incident neutron momentum in vacuum. For the case where the scattering length density varies through the thickness of a film deposited on a substrate, the reflectivity can be modeled by dividing the film into j layers of an arbitrary thickness d_j and scattering length density $(b/V)_j$. If the substrate is designated as the $j+1$ layer, the reflectance at the substrate is given by

$$r'_{j,j+1} = (k_{z,j} - k_{z,j+1})/(k_{z,j} + k_{z,j+1}) \tag{2}$$

while at the interface between the layer adjacent to the substrate and the $j-1$ layer

$$r_{j-1,j} = \frac{r'_{j-1,j} + r'_{j,j+1}\exp(2id_jk_{z,j})}{1 + r'_{j-1,j}r'_{j,j+1}\exp(2id_jk_{z,j})} \tag{3}$$

The reflectance at the j–2, j–1 interface is calculated recursively as

$$r_{j-2,j-1} = \frac{r'_{j-2,j-1} + r_{j-1,j}\exp(2id_{j-1}k_{z,j-1})}{1 + r'_{j-2,j-1}r_{j-1,j}\exp(2id_{j-1}k_{z,j-1})} \tag{4}$$

Following this recursion through the j layers, the reflectance at the film surface $r_{0,1}$ can be obtained.[13-16] The reflectivity is then defined as

$$R(k_{z,0}) = r_{0,1}r_{0,1}^* \tag{5}$$

where the asterisk denotes the complex conjugate. In-

Table II
Constants Used in Calculations

material	density (g/cm³)	(b/V) (×10⁻⁶ Å⁻²)	material	density (g/cm³)	(b/V) (×10⁻⁶ Å⁻²)
PMMA	1.15	1.0	d-PS	1.14	6.1
d-PMMA	1.24	6.8	Si	2.32	2.08
PS	1.06	1.43	SiO_2	2.20	3.48

strumental resolution is incorporated within the calculation of the reflectivity by convolving the reflectivity with a Gaussian function defining the resolution.

For an ordered copolymer/homopolymer film in which one copolymer block is deuterated and the homopolymer labeling matches that of the corresponding copolymer block, the model for the scattering length density profile is straightforward, assuming complete segregation of the homopolymer to like domains. In such cases, the reflectivity profile is typically described by a model that consists of alternating layers having the b/V values of the deuterated and hydrogenated components, with a characteristic hyperbolic tangent interface between the PS and PMMA domains which can be incorporated into the recursion relations.[11,12] Scattering length density values for materials relevant to this study are given in Table II.

When deuterated homopolymer is added to the unlabeled copolymer, the scattering length density profile is more complex, and some form for the homopolymer distribution must be assumed. For these systems, the copolymer domains that contain the homopolymer are divided into incremental layers typically 5 Å in thickness. The b/V value for each layer is then calculated from a model concentration profile in which the homopolymer is distributed about the center of the domain and decays to some base value at the domain boundaries. The model thus encompasses two extremes for incorporating a given homopolymer concentration within the domain: (1) the homopolymer can be entirely confined to the domain center, represented by a narrow Gaussian distribution, or (2) the homopolymer can be uniformly distributed through the domain, such that the scattering length density of each layer in the domain is equal to the average b/V value for the domain. The model additionally incorporates a hyperbolic tangent interfacial profile between PS and PMMA layers. The homopolymer is assumed to be confined to like domains. This assumption is supported by the results obtained for compositionally equivalent strong-scattering systems (see Table I). Model parameters, including the full-width half-maximum, base value, and total value of the homopolymer concentration in each domain, the domain widths, and the interfacial thicknesses, were determined using an interactive fitting procedure to minimize the absolute difference between the calculated reflectivity curves and the experimental data. Because the weak-scattering systems are effectively composed of three components, interfacial widths and layer thicknesses cannot be uniquely determined. For this reason large errors are listed for the average domain widths in these systems (Table III). The average lamellar spacing, however, is expected to be accurate to within ± 5 Å for most samples.

IV. Results and Discussion

Figures 1 and 2 show the reflectivity profiles for 101K P(d-S-*b*-MMA) blended with 5 and 10 wt % 64K PMMA, samples DH1 and DH2. The strong Bragg reflections which are evident in the profiles indicate that a high degree of ordering is present parallel to the substrate. The circles represent the experimental data, while the solid line is the reflectivity calculated from the scattering length density profile shown in the inset. (Error bars on the experimental data fall within the circles.) The decrease in the reflectivity observed at low momentum values below the critical angle is a consequence of the finite sample size.[11] As evidence by the model b/V profile shown in the inset, the PMMA homopolymer appears to segregate completely to the

Table III
Parameters Derived from the Reflectivity Profiles

sample	description	d_s (Å)	d_m (Å)	d (Å)	a_I (Å)
HH0	P(S-*b*-MMA) 91K	176 ± 2	200 ± 6	376 ± 5	52 ± 12
HH1	+5% d-PMMA 57K	196 ± 10	219 ± 10	415 ± 5	52[a]
HH2	+5% d-PMMA 57K +5% PS 52K	202 ± 10	218 ± 10	420 ± 5	52[a]
HH3	+10% d-PMMA 57K	189 ± 10	236 ± 10	425 ± 5	49[a]
HH4	+10% d-PMMA 12K	166 ± 10	219 ± 10	385 ± 5	51[a]
HH5	+5% d-PS 50K	216 ± 5	200 ± 5	416 ± 5	52[a]
HH6	+10% d-PS 50K	214 ± 5	191 ± 5	405 ± 5	56[a]
HH7	+5% d-PS 500K	181 ± 5	206 ± 5	387 ± 5	76 ± 8
HH8	+10% d-PS 500K	179 ± 5	209 ± 10	388 ± 10	66 ± 20
DH0	P(d-S-*b*-MMA) 101K	206 ± 3	188 ± 2	394 ± 3	50 ± 5
DH1	+5% PMMA 64K	200 ± 1	208 ± 1	408 ± 1	48 ± 4
DH2	+10% PMMA 64K	203 ± 1	233 ± 2	436 ± 2	49 ± 8
DH3	+10% PMMA 9.2K	179 ± 1	209 ± 3	388 ± 3	57 ± 6
DH4	+5% d-PS 50K	216 ± 3	187 ± 1	403 ± 2	55 ± 3
DH5	+10% d-PS 50K	230 ± 2	184 ± 1	414 ± 2	64 ± 8
DH6	+5% d-PS 500K	210 ± 1	193 ± 1	403 ± 1	57 ± 7
DH7	+10% d-PS 500K	208 ± 2	194 ± 2	402 ± 2	71 ± 9

[a] Values were restricted to within the limits set by the strong-scattering equivalents.

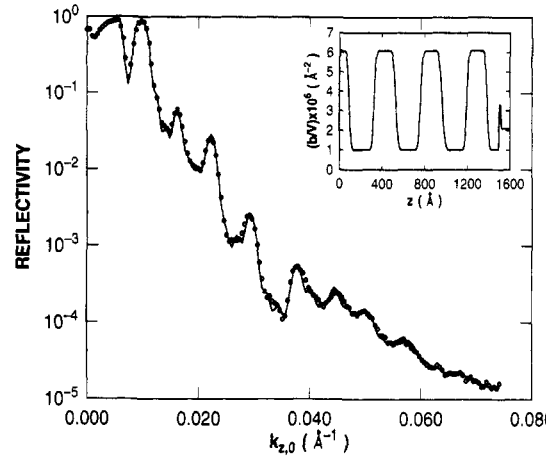

Figure 1. Neutron reflectivity profile for blend DH1, 95 wt % P(d-S-*b*-MMA) 101K copolymer with 5 wt % PMMA 64K homopolymer. In this figure as in the remaining figures, the circles represent experimental data. Solid curve is the calculated reflectivity profile using the scattering length density profile shown in the inset.

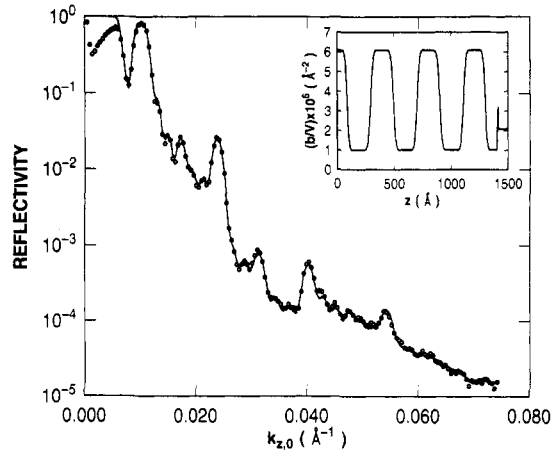

Figure 2. Neutron reflectivity profile for blend DH2, 90 wt % P(d-S-*b*-MMA) 101K copolymer with 10 wt % PMMA 64K homopolymer. Solid curve is the calculated reflectivity profile using the scattering length density profile shown in the inset.

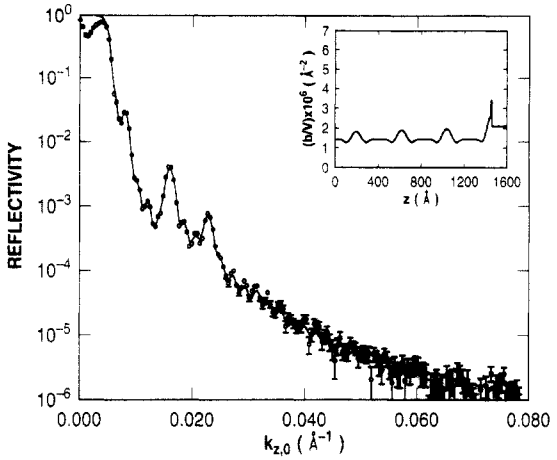

Figure 3. Neutron reflectivity profile for blend HH2, 95 wt % P(d-S-*b*-MMA) 91K copolymer with 5 wt % d-PMMA 57K homopolymer. Solid curve is the calculated reflectivity profile using the scattering length density profile shown in the inset.

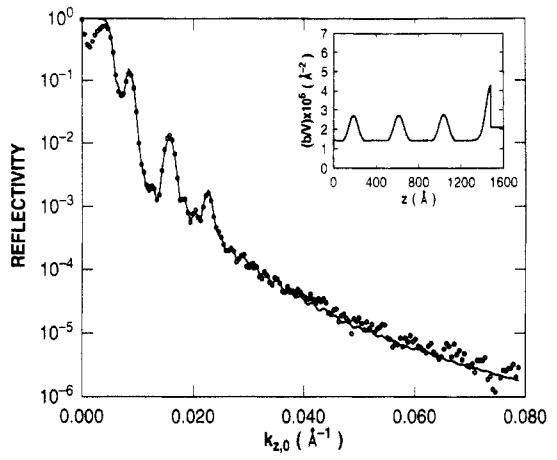

Figure 4. Neutron reflectivity profile for blend HH3, 90 wt % P(S-*b*-MMA) 91K copolymer with 10 wt % d-PMMA 57K homopolymer. Solid curve is the calculated reflectivity profile using the scattering length density profile shown in the inset.

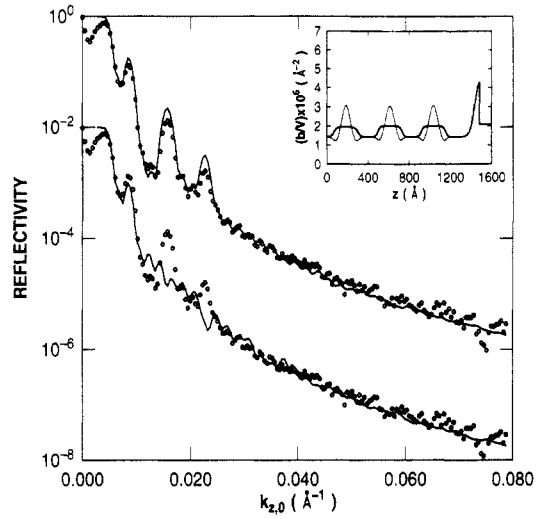

Figure 5. Calculated reflectivity profiles for blend HH3. The upper curve assumes a more centralized homopolymer distribution (thin line in b/V inset) than is indicated in Figure 4. The lower curve assumes a completely uniform distribution of homopolymer in the PMMA domains (thick line in b/V inset). The PMMA half-layer at the substrate was not altered.

PMMA domains of the multilayered structure. With increasing homopolymer content, the average lamellar period increases due to an expansion of the PMMA domains, while the average thickness of the PS layers decreases only slightly, by 2 or 3% (Table III). These results are in accord with those of Winey et al.[8] for blends of a symmetric 49K poly(styrene-*b*-isoprene) diblock with 37K polystyrene. While the lamellar period increases 4 and 10% for the DH1 and DH2 blends relative to the pure copolymer, sample DH0, the homopolymer addition does not significantly affect the average interfacial width between PS and PMMA layers. These combined observations suggest that, for these blends, the homopolymer has little influence on the chain configurations of the PS blocks.

As observed for pure P(S-*b*-MMA) diblock copolymers,[11,12] thin films of symmetric diblocks blended with PMMA (or PS) homopolymer order such that PS, the lower surface energy component, forms a half-layer at the film surface. At the Si interface a half-layer of PMMA is found due to a favorable interaction between PMMA and the oxide layer which forms on the silicon surface, typically 15 Å in thickness. In the scattering length density profiles shown in Figures 1 and 2, this oxide layer has been incorporated into the model, using a b/V value of $\sim 3 \times 10^{-6}$ Å^{-2}. These results additionally show that, as with pure block copolymers,[10,11,16] the blends order such that the equilibrium thickness of the system is quantized to $(n + 1/2)$ layers, where n is an integer. If the thickness of the film when originally cast does not correspond closely to $(n + 1/2)$ layers, the copolymer satisfies this condition by the formation of integral steps or holes on the surface of the film. Several recent studies have examined this phenomenon using optical microscopy and atomic force microscopy.[17-19]

While the results in Figures 1 and 2 might yield a qualitative picture of the homopolymer distribution within the PMMA domains, a quantitative description is only possible if contrast is achieved between the homopolymer and copolymer components. Figures 3 and 4 show the reflectivity data for unlabeled 91K P(S-*b*-MMA) blended with 57K d-PMMA in concentrations of 5 and 10 wt %, samples HH2 and HH3, respectively. (Error bars have been included in Figure 3 for completeness but have been excluded from the remainder of the figures for purposes of clarity.) Multiple Bragg reflections are again observed in both profiles, reaffirming the segregation of homopolymer to the PMMA domains. The low peak intensities, however, reveal significant intermixing between the unlabeled PMMA copolymer blocks and the labeled homopolymer within the PMMA domains. The scattering length density profiles used to generate the model reflectivity curves are shown in the insets. In both figures, centralization of the homopolymer within the PMMA domains is apparent. In addition, both profiles suggest that excess homopolymer resides in the PMMA layer adjacent to the substrate.

The sensitivity of the reflectivity measurements to the homopolymer distribution is demonstrated in Figure 5, which shows calculated reflectivities for the 10 wt % blend, sample HH3, assuming a completely uniform distribution (bottom curve) and a more centralized distribution (top curve) within the PMMA layers, keeping the fraction of homopolymer in each layer constant. (The half-layer adjacent to the substrate, which governs the reflectivity at high angles, was not altered.) In examining this figure it is clear that the homopolymer distribution must be centralized and that the reflectivity is quite sensitive to the peak concentration of the homopolymer within the ordered domains.

Because blends HH2 and HH3 are effectively three-component systems, i.e., they contain materials with three distinct b/V values, volume fractions cannot be calculated uniquely from the scattering length density profiles in

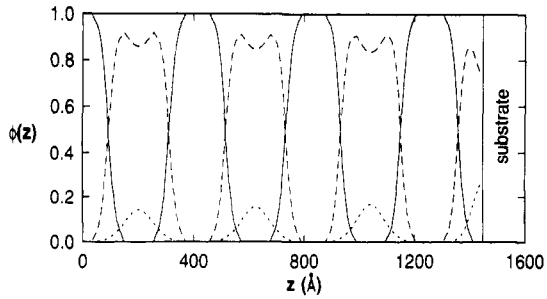

Figure 6. Volume fraction profile for PS (solid), PMMA (dashed), and d-PMMA (dotted) components in blend HH2, obtained from the scattering length density inset in Figure 3.

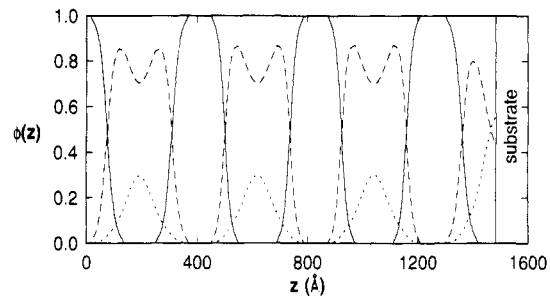

Figure 7. Volume fraction profile for PS (solid), PMMA (dashed), and d-PMMA (dotted) components in blend HH3, obtained from the scattering length density inset in Figure 4.

Figures 3 and 4. Therefore, several assumptions were introduced based on results from the strong-scattering analogues in Figures 1 and 2, DH1 and DH2, respectively. The reflectivity profiles for the HH2 and HH3 blends, though sensitive to the total lamellar period, are somewhat insensitive to the thickness of the PS and PMMA domains. Therefore, initial values for these parameters used in the fitting procedure were forced to be consistent with the results for the strong-scattering blends. The large confidence limits for the domain widths listed in table III are a reflection of this biasing in the fits. In addition, the interfacial thickness between PS and PMMA layers was restricted within limits set by the average values obtained for the strong-scattering systems (45–55 Å). It should be noted that for sample HH3 a ~4% 42K homopolystyrene impurity was not removed from the diblock prior to sample preparation, while for sample HH2, 5 wt % 52K polystyrene was intentionally introduced in the system. The PS domain widths are, therefore, significantly larger than the value for the purified 91K copolymer, sample HH0. Based on results for the strong scattering blend, DH4, the polystyrene impurity is expected to have a negligible effect on the PMMA domain widths at this concentration level. For both weak-scattering samples, the relative volume fraction of PMMA given by the ratio of the width of the PMMA domain, d_m, to the total period, d, i.e., d_m/d, is consistent with the value calculated from the initial blend composition (Table I).

Figures 6 and 7 show the volume fraction profiles obtained from the scattering length density profiles shown in the insets of Figures 3 and 4. As can be seen, the PMMA homopolymer (dotted curve) is sandwiched between PMMA copolymer blocks (dashed curve). For both blends the maxima in the homopolymer distributions are roughly twice the average volume fraction of homopolymer in the PMMA domains, ~9% for HH2 and 17% for HH3. An excess of homopolymer at the interface between the film and the substrate is seen in both profiles. The homopolymer coverage at the Si surface is nearly twice the peak homopolymer concentration for the internal layers. Still, the homopolymer chains are seen to penetrate well into the interfacial regions in both systems. The homopolymer

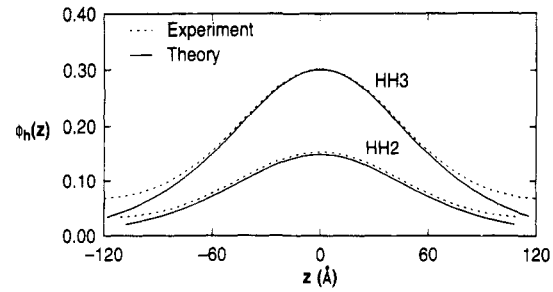

Figure 8. Comparison of homopolymer distributions: (- - -) experimental; (—) mean-field results of Shull and Winey.[9] Dashed curves are distributions from representative domains of blends HH2 and HH3. Solid curves were calculated from eqs 6 and 7, with parameters given in the text.

volume fraction, φ_h, determined from the average domain concentration, φ_m, domain width, and lamellar spacing, $\varphi_h = \varphi_m d_m/d$, compares well in each case with the homopolymer volume fraction calculated from the blend composition, using the densities listed in Table II. Integrated over the total film thickness, however, the homopolymer volume fractions are somewhat overestimated as 4.9% for HH2 and 10.7% for HH3. This discrepancy arises, most likely, from the inability to distinguish the oxide layer on the silicon surface from the deuterated homopolymer present. In fitting sample HH2, an 11-Å oxide layer was incorporated in the profile, while for HH3, the oxide layer was neglected. Thus, particularly in Figure 7, the homopolymer excess in the PMMA half-layer is probably overestimated. The homopolymer content in the layers, however, should closely approximate the true value since the fit is quite sensitive to the maxima in the b/V profiles.

A recent mean-field treatment by Shull and Winey[9] simulates homopolymer distributions within lamellar diblock copolymer morphologies based on an earlier model for polymer brushes.[20,21] The analysis assumes that the homopolymer chains are entirely confined within like copolymer domains and that the boundaries between adjacent domains are infinitely sharp. For systems in which the homopolymer molecular weight is greater than or comparable to the molecular weight of the corresponding copolymer block, a simple analytical form is derived for the homopolymer distribution across the domain:[9]

$$\varphi_h(z) = 0.5\left\{\tanh\left(\frac{\varphi_A d_A + 2z}{w_0}\right) + \tanh\left(\frac{\varphi_A d_A - 2z}{w_0}\right)\right\} \quad (6)$$

where φ_A is the total volume fraction of homopolymer in the A domain, d_A is the domain width, and w_0 characterizes the overlap between copolymer brushes anchored at the domain wall and the homopolymer chains localized to the domain center. When the homopolymer molecular weight is greater than the block molecular weight, w_0 can be approximated from an empirical form obtained for infinite homopolymer molecular weight:

$$w_0 = 1.09R_g + 3.16[R_g^2/(1-\varphi_A)d_A] \quad (7)$$

where $R_g = N_A^{1/2} l_A/\sqrt{6}$ is the unperturbed radius of gyration of a copolymer block with N_A segments of length l_A. From eqs 6 and 7, volume fraction profiles can be generated to compare with those in Figures 6 and 7. For the 91K copolymer used in this study, $N_{PMMA} \approx 500$. The segment length for PMMA was taken to be 6.85 Å.[11,22]

In Figure 8 is shown the calculated distribution (solid curve) for a domain thickness of 218 Å and a homopolymer content of 9.0 vol % compared to the fitted distribution for the corresponding HH2 domain (dashed curve). Since the mean-field treatment assumes a sharp boundary

between PS and PMMA layers, the PMMA concentration in Figure 6 was normalized to one within the interfacial regions. The two results are in very good agreement. Near the domain boundaries, however, the mean-field analysis appears to underestimate the homopolymer concentration. Indeed, the normalized area under the calculated curve does not equate to the input concentration, φ_A. Integrating eq 6 over the domain width d_A using the approximation in (7), one finds that material conservation is strictly achieved only in the continuous chain limit, $l_A \rightarrow 0$. This discrepancy is more apparent on comparing the calculated and experimental distributions in Figure 8 for the HH3 blend using a domain width of 237 Å and a homopolymer content of 17.2 vol %. Nevertheless, the analytic expressions given in eqs 6 and 7 provide a very good approximation of the observed distributions when the homopolymer molecular weight is comparable to that of the corresponding copolymer block. For lower molecular weight homopolymers, the copolymer brush profiles will depend upon the ratio of the homopolymer molecular weight to that of the copolymer, and the simple analytic form used above is not applicable.[9] A mean-field treatment for such cases is beyond the scope of the present study and will be discussed in a future communication.

For low molecular weight homopolymers incorporated into ordered copolymer domains, intermixing of the homopolymer chains with the copolymer blocks is entropically favored. Therefore, the homopolymer distribution across the domain is more uniform.[7,8] In sample DH3, labeled copolymer DH0 is blended with 10 wt % 9.2K PMMA homopolymer. With the improved interpenetration of homopolymer and copolymer, the PMMA domain expansion is less dramatic than that observed for the 64K homopolymer blend DH2 (see Table III). Swelling of the PMMA blocks by short homopolymer chains increases the average distance between PS–PMMA junction points along the interface. This produces a larger contraction of the adjacent PS domains, in order to preserve constant density in these layers. This pronounced effect yields a slight decrease in the average lamellar spacing relative to the pure copolymer. These observations are consistent with results from recent small-angle scattering studies by Hashimoto et al.[7] and Winey et al.[8] The reflectivity analysis additionally suggests that swelling the PMMA brushes with short homopolymer chains broadens the interfacial region between PS and PMMA layers.

Comparing the results of the reflectivity analyses for samples DH2 and DH3 suggests that the lower molecular weight homopolymer is more uniformly distributed within the PMMA domains. A more quantitative comparison can be made, however, by analyzing the reflectivity profile in Figure 9 (top curve) for a blend of unlabeled copolymer with 10 wt % 12K d-PMMA homopolymer, sample HH4. In this profile the higher order reflections are absent, while the first-order reflection is significantly lower than that of the 57K blend HH3 in Figure 4. Although the system is well ordered, the contrast between the PS and PMMA domains is much lower, indicating that the homopolymer chains and PMMA blocks are highly intermixed within the PMMA domains. At larger $k_{z,0}$, the reflectivity is significantly higher than for the previous system, resulting from a higher concentration of labeled homopolymer at the interface between the film and substrate. From the model b/V profile shown in the inset of Figure 9, the corresponding volume fraction profile in Figure 10 was calculated. The homopolymer coverage at the substrate is shown to be above 80%.

While the results in Figures 9 and 10 clearly point to a significant intermixing of the labeled and unlabeled PMMA segments, the scattering length density profile in

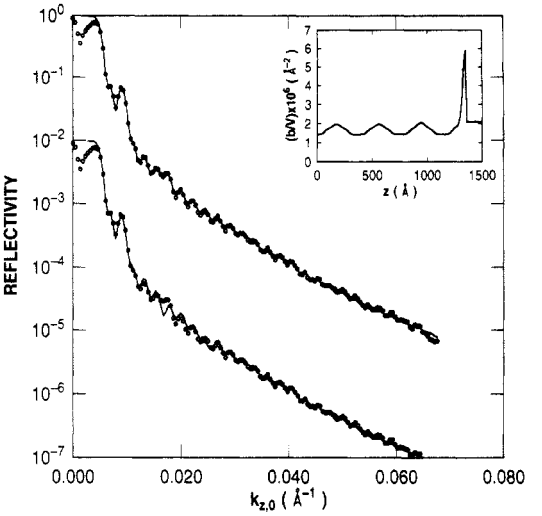

Figure 9. Reflectivity profile for blend HH4, 90 wt % P(S-*b*-MMA) 91K copolymer with 10 wt % d-PMMA 12K homopolymer. Upper curve shows the calculated reflectivity profile using the b/V profile given in the inset. Lower curve shows the calculated reflectivity profile for a completely uniform distribution of homopolymer in the internal PMMA layers (the half-layer at the substrate interface was not altered).

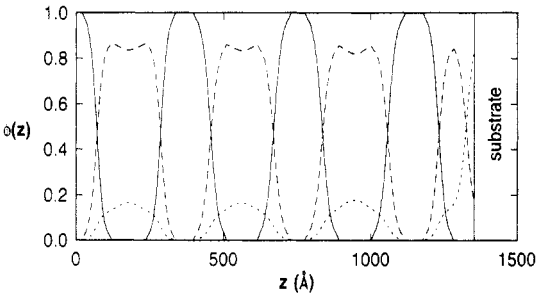

Figure 10. Volume fraction profile for PS (solid), PMMA (dashed), and d-PMMA (dotted) components in blend HH4, obtained from the scattering length density inset in Figure 9.

the inset of Figure 9 and the volume fraction profile in Figure 10 suggest that the homopolymer concentration is still slightly higher at the center of PMMA domains. To substantiate this conclusion, the reflectivity profile was calculated assuming a uniform distribution of the homopolymer in the three PMMA layers. The comparison to the experimental data is shown in the bottom of Figure 9 (this has been offset for clarity). While the calculated profile captures most features of the experimental data, there is clear disagreement between the calculated curve and the data in the momentum range from 0.015 to 0.02 Å^{-1}. This demonstrates that the distribution cannot be uniform and emphasizes the sensitivity of neutron reflectivity to the spatial distribution of labeled homopolymer.

The average homopolymer content in the PMMA domains yields an estimated value for the homopolymer volume fraction of $\varphi_h = \varphi_m d_m/d = 0.081$, which falls somewhat short of the calculated value of 0.09 for this blend composition. Integrated over the total film thickness, however, the homopolymer fraction of 0.10 overestimates the calculated value by 0.01. Again, however, the inability to resolve the labeled homopolymer from the oxide at the Si surface is the most logical explanation for this discrepancy.

The excess homopolymer which resides at the substrate in samples HH2, HH3, and HH4 might suggest the thermodynamic coexistence of a homopolymer-rich disordered phase along with the ordered lamellar phase. This is unlikely, however, particularly for blends HH2 and HH4. For these systems, the annealing temperature is well above

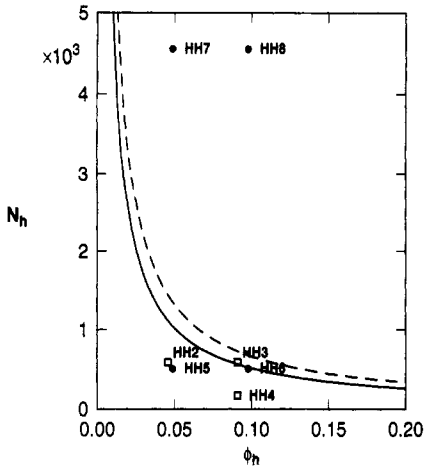

Figure 11. Mean-field spinodal curves for macrophase separation of P(S-*b*-MMA) 91K copolymer and PMMA (dashed curve) or PS (solid curve) homopolymers as a function of homopolymer concentration φ_h and number of segments N_h. Open squares indicate blends with added d-PMMA. Filled circles indicate blends with added d-PS. The 42K homopolymer impurity not extracted from the copolymer (~4%) was not taken into account (see Table I).

the stability limit for phase separation of the copolymer and PMMA homopolymer obtained from the Flory–Huggins free energy of mixing:[23]

$$\Delta F/kT = \frac{\varphi_h}{N_h} \ln \varphi_h + \frac{1-\varphi_h}{N} \ln (1-\varphi_h) + \chi_{sm} f_s^2 \varphi_h (1-\varphi_h) \tag{8}$$

where N_h is the number of segments per PMMA homopolymer chain, f_s is the volume fraction of PS in the block copolymer, and χ_{sm} is the interaction parameter for styrene and methyl methacrylate:[22]

$$\chi_{sm} = 0.028 + 3.9/T \tag{9}$$

where T is the absolute temperature. At the annealing temperature of 160 °C, $\chi_{sm} = 0.037$. The stability limit or spinodal is defined from (8) as $\partial^2 \Delta F/\partial \varphi_h^2 = 0$. In Figure 11 the spinodal is plotted as a function of PMMA (solid curve) or PS (dashed curve) homopolymer concentration and molecular weight for copolymer HH0, using $\chi_{sm} = 0.037$. In this figure blends HH2 ($N_h = 530$, $\varphi_h = 0.045$) and HH4 ($N_h = 110$, $\varphi_h = 0.090$) fall well outside the spinodal, while sample HH3 ($N_h = 530$, $\varphi_h = 0.090$) is somewhat closer to the stability limit. For higher concentrations at this molecular weight, partial exclusion of the homopolymer from the ordered copolymer domains might result. This could explain the anomalous values for the average domain widths and lamellar spacing determined for the HH6 blend, which contains 10 wt % 50K d-PS along with the 42K polystyrene impurity (~4% of the unpurified diblock volume) not removed prior to sample preparation.

For much higher molecular weights, the homopolymer solubility drops appreciably and macroscopic phase separation is anticipated. In this study we examined the thin-film morphology of copolymers HH0 and DH0 blended with 500K d-PS homopolymer. For this molecular weight ($N_h = 4500$), a 5 or 10 wt % homopolymer concentration falls well within the two-phase region of Figure 11. Upon annealing, however, these films remained transparent, and optical microscopy revealed no evidence for macroscopic phase separation. In fact, island or hole formation on the surface of the film was observed, indicating a retention of the lamellar ordering parallel to the substrate.

Figure 12 shows the reflectivity profile for sample DH7, a blend of DH0 copolymer with 10 wt % 500K deuterated

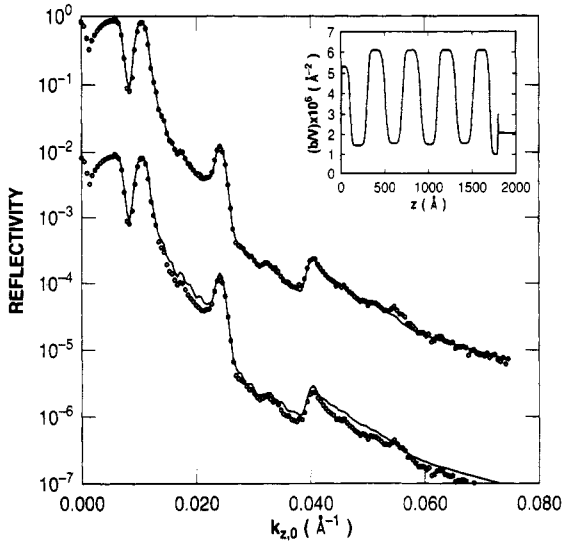

Figure 12. Reflectivity profile for blend DH7, 90 wt % P(d-S-*b*-MMA) 101K copolymer with 10 wt % d-PS 500K homopolymer. Upper curve shows the calculated reflectivity profile using the b/V profile given in the inset. Lower curve shows the calculated reflectivity profile using the full b/V value for d-PS in the surface half-layer of the scattering length density profile.

polystyrene. The solid line (upper curve) is the best fit to the experimental data using the scattering length density profile shown in the inset. Again, a periodic variation in the scattering length density through the entire film is found, demonstrating that the multilayered structure has been maintained. The low scattering length density value for the PS half-layer at the air surface is indicative of the formation of islands on the free surface,[17-19] and the scattering length density at the surface is a weighted sum of the scattering length density for the underlayer and air ($b/V = 0$).[15] Using the full b/V vlaue for the half-layer at the surface, i.e., assuming no islands, results in the lower curve in Figure 12. As can be seen, the agreement between the measured and calculated profiles is not as good, although the average domain size and spacing are still captured.

In contrast to sample DH5 where 10 wt % d-PS 50K was added, the lamellar spacing for DH7 is not appreciably larger than that for the pure copolymer. The width of the polystyrene domains is seen to remain approximately constant, indicating exclusion of the homopolymer. The average PMMA domain width increases slightly (~3%), while the interphase widths are notably larger. In addition, the scattering length density of the PMMA layers required to fit the data (~1.5×10^{-6} Å^{-2}) was significantly higher than that of pure PMMA (1.5×10^{-6} Å^{-2}). These results suggest a multilayered morphology having small localized domains of homopolymer distributed throughout the film rather than a coarse, macroscopic phase separation of the homopolymer to the surface or into large homopolymer-rich domains. Consequently, the scattering length density of the PMMA layers represents a local average of 90% PMMA with 10% d-PS. The broadening of the interfacial region is also consistent with a model of localized homopolymer segregation, whereby the near-perfect layering of the lamellar domains is compromised locally to accommodate the homopolymer. Consistent with the brush/homopolymer profiles characterized by eqs 6 and 7, PS copolymer brushes would effectively sandwich the PS homopolymer bridging through the PMMA layers. This would increase the number of joints per unit area of PS/PMMA interface, thereby causing an increase in the width of the PMMA domains to maintain constant density.

To investigate this point further, electron microscopy was performed on thin films of the DH7 mixture. Here,

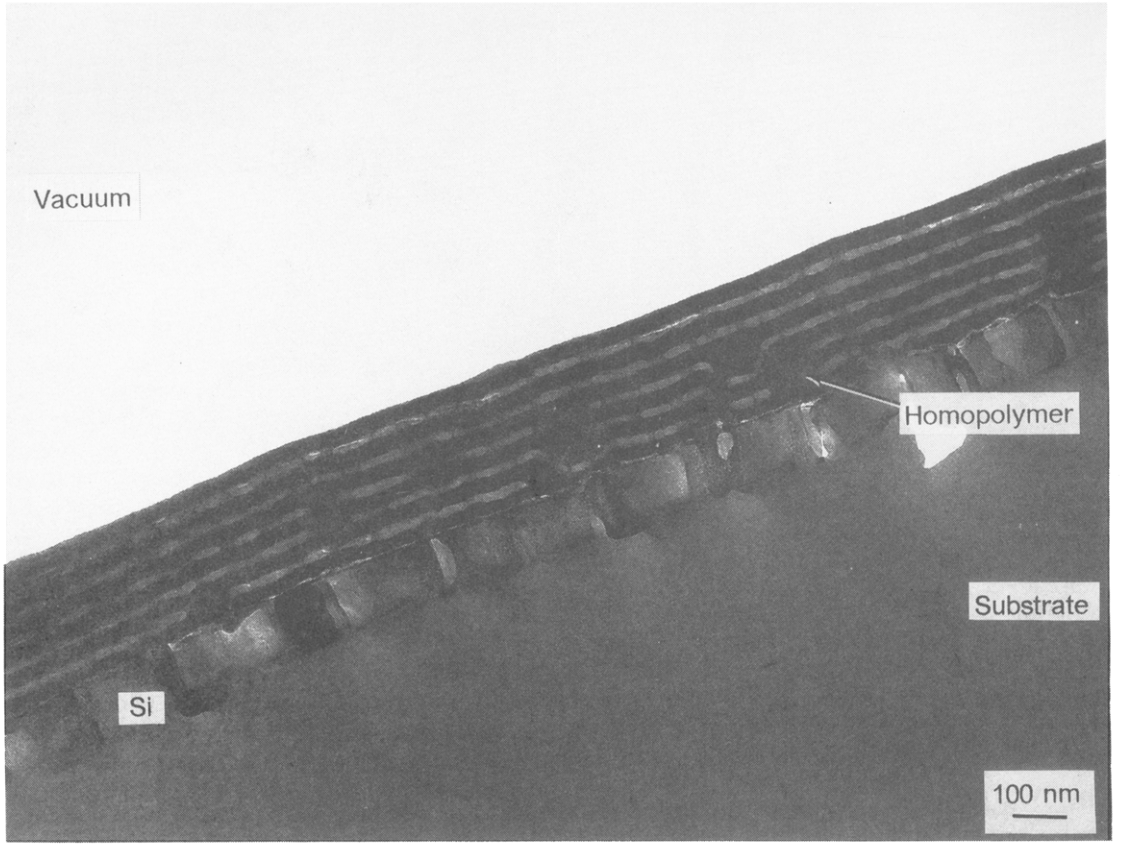

Figure 13. Electron micrograph of the DH7 mixture containing 10% 500K d-PS. The sample was prepared on an Ultem polyimide substrate coated with Si. The sample was microtomed normal to the surface and stained with RuO_4 vapors, which preferentially stain the polystyrene (dark regions). The magnification is indicated in the figure.

specimens were prepared by spin casting the mixture onto a substrate consisting of a thick polyimide (Ultem) sheet coated with a thin (~1000 Å) film of evaporated Si. The specimens were annealed for 5 days under vacuum in a manner identical to that used for the reflectivity studies. The use of the polyimide substrate permitted microtoming could be seen. The microtomed specimen was stained with RuO_4, which preferentially stains the polystyrene. Figure 13 shows a typical micrograph for the DH7 mixture. The micrograph is quite dramatic. While one can not distinguish between the PS of the homopolymer or copolymer, localized pockets of PS are scattered throughout the film. Remarkably, the multilayered structure is maintained and the homopolymer domains are incorporated with little distortion to the orientation of the multilayers. It also appears that there is no preferential segregation of the homopolymer to either the air or substrate interface. Thus, the conclusions drawn from the reflectivity measurements are in good agreement with the electron microscopic observations.

The above conclusions are supported by the reflectivity profiles from blends of unlabeled copolymer with labeled high molecular weight homopolymer. Figure 14 shows the reflectivity profile for HH0 blended with 5 wt % 500K d-PS, sample HH7. This figure can be compared with the reflectivity profile in Figure 15 for a blend of this copolymer with 5 wt % 50K d-PS sample HH5. The two profiles are qualitatively similar. Each suggests a slight homopolymer excess at the film surface. For sample HH7, however, the Bragg reflections are less pronounced, indicating lower contrast between the PS and PMMA domains. From the scattering length density profile used to fit the reflectivity data, the homopolymer distribution in this system appears to be nearly uniform across the width of the PS layers, while in HH5, the homopolymer is centralized within the

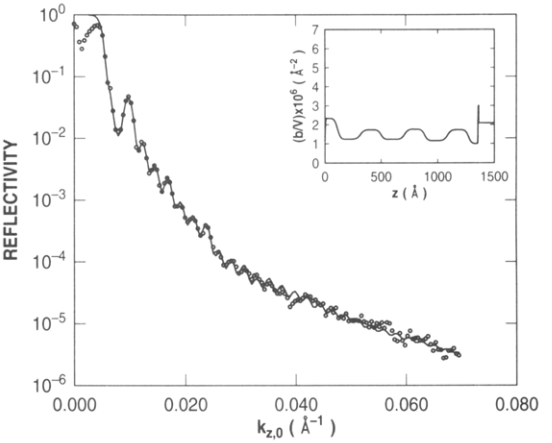

Figure 14. Neutron reflectivity profile for blend HH7, 95 wt % P(S-*b*-MMA) 91K copolymer with 5 wt % d-PS 500K homopolymer. Solid curve is the calculated reflectivity profile using the scattering length density profile shown in the inset.

PS domains. In the HH7 blend, the PS domain width is again effectively unchanged, while the PMMA domain width increases slightly, in agreement with the results for DH6 and DH7. The volume fraction distributions determined from the scattering length density profiles for samples HH5 and HH7 are shown in Figures 16 and 17.

The homopolymer concentration integrated over the film thickness is 4.5 vol % for sample HH5, in good agreement with actual concentration of 4.8%. For HH7, however, the integrated homopolymer content is somewhat higher at 6.1 vol %. Comparing Figure 16 with Figure 6, the 50K d-PS homopolymer appears to be less centralized in the domains than the 57K d-PMMA homopolymer. This result is supported by the increase in the interfacial width observed for the strong-scattering systems, DH4 and DH5.

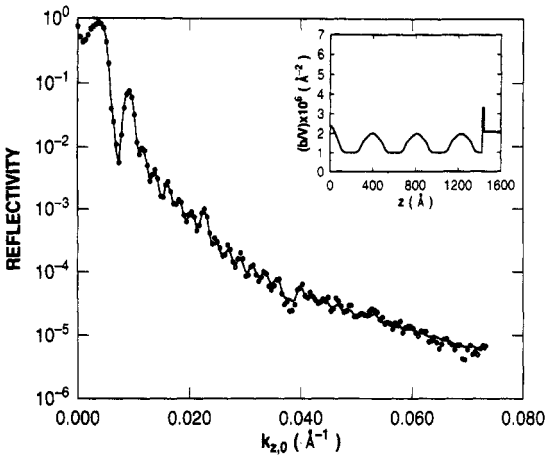

Figure 15. Neutron reflectivity profile for blend HH5, 95 wt % P(S-*b*-MMA) 91K copolymer with 5 wt % d-PS 50K homopolymer. Solid curve is the calculated reflectivity profile using the scattering length density profile shown in the inset.

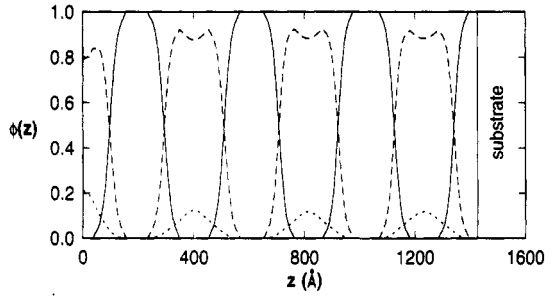

Figure 16. Volume fraction profile for PMMA (solid), PS (dashed), and d-PS (dotted) components in blend HH5, obtained from the scattering length density inset in Figure 14.

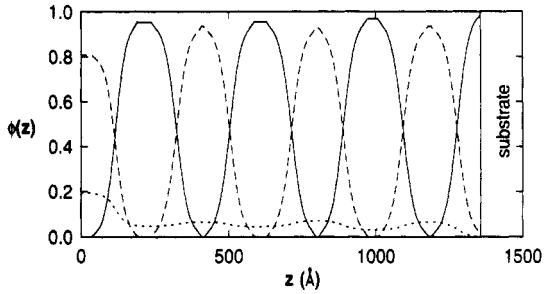

Figure 17. Volume fraction profile for PMMA (solid), PS (dashed), and d-PS (dotted) components in blend HH7, obtained from the scattering length density inset in Figure 13.

V. Conclusions

In this study neutron reflectivity has been used to obtain detailed descriptions of homopolymer distributions in ordered symmetric copolymers not measurable by other techniques. For homopolymer molecular weights comparable to that of the corresponding copolymer block, the mean-field treatment by Shull and Winey[9] gives a good approximation for the observed distributions. For low molecular weights, the homopolymer is distributed almost uniformly within the corresponding domains. When PMMA is added to the copolymer, an excess of homopolymer is present at the substrate, while for PS homopolymer addition, an excess is observed at the surface. While these observations may possibly be attributed to deuteration effects,[24] it is also possible that the presence of excess homopolymer relaxes the geometrical constraints placed on the copolymer brushes at the boundaries of the film.

When high molecular weight homopolymer is added to the copolymer, the homopolymer segregates to relatively small domains distributed throughout the film. The phase separation of the homopolymer and copolymer, which apparently is arrested by the ordering process of the copolymer, does not significantly disrupt the final lamellar orientation. An analysis of the off-specular scattering might provide insight on the in-plane correlations for these morphologies.

Acknowledgment. The authors are indebted to Dr. M. Kunz for obtaining the micrograph in Figure 13. It was reassuring to find our conclusions from the reflectivity profiles were correct. We would also like to thank Dr. K. Shull for stimulating discussions during the course of this work. This work was supported, in part, by the Department of Energy, Office of Basic Energy Sciences, under Contract DE-FGO3-88ER45375.

References and Notes

(1) Hasegawa, H.; Tanaka, H.; Yamasaki, K.; Hashimoto, T. *Macromolecules* **1987**, *20*, 1651.
(2) Thomas, E. L.; Anderson, D. M.; Henkee, C. S.; Hoffman, D. *Nature* **1988**, *334*, 598.
(3) *Developments in Block Copolymers—I*; Goodman, I., Ed.; Applied Science: New York, 1985.
(4) Winey, K. I.; Thomas, E. L.; Fetters, L. J. *Macromolecules* **1992**, *25*, 2645.
(5) Roe, R. J.; Zin, W.-C. *Macromolecules* **1984**, *17*, 89.
(6) Ptaszynaski, B.; Terrisse, J.; Skoulios, A. *Makromol. Chem.* **1975**, *176*, 3483.
(7) Hashimoto, T.; Tanaka, H.; Hasegawa, H. *Macromolecules* **1990**, *23*, 4378.
(8) Winey, K. I.; Thomas, E. L.; Fetters, L. J. *Macromolecules* **1991**, *24*, 6182.
(9) Shull, K. R.; Winey, K. I. *Macromolecules* **1992**, *25*, 2637.
(10) Quan, X.; Gancarz, I.; Koberstein, J. T.; Wignall, G. D. *Macromolecules* **1987**, *20*, 1434.
(11) Anastasiadis, S. H.; Russell, T. P.; Satija, S. K.; Majkrzak, C. F. *Phys. Rev. Lett.* **1989**, *62*, 1852.
(12) Anastasiadis, S. H.; Russell, T. P.; Satija, S. K.; Majkrzak, C. F. *J. Chem. Phys.* **1990**, *92*, 5677.
(13) Werner, S. A.; Klein, A. G. In *Neutron Scattering*; Price, D. L., Skold, A., Eds.; Academic Press: New York, 1989.
(14) Als-Nielsen, J. In *Structure and Dynamics of Surfaces—II*; Schommers, M., Blanchenhagen, Von P., Eds.; Springer-Verlag: Berlin, 1987.
(15) Russell, T. P. *Mater. Sci. Rep.* **1990**, *5*, 171.
(16) Heavens, O. S. *Optical Properties of Thin Solid Films*; Dover Press: New York, 1965.
(17) Coulon, G.; Russell, T. P.; Deline, V. R.; Green, P. F. *Macromolecules* **1989**, *22*, 2581.
(18) Coulon, G.; Collins, B.; Ausserre, D.; Chatenay, D.; Russell, T. P. *J. Phys. Fr.* **1990**, *52*, 2801.
(19) Collin, B.; Chatenay, D.; Coulon, G.; Ausserre, D.; Gallot, Y. *Macromolecules* **1992**, *25*, 1621.
(20) Shull, K. R.; Kramer, E. J. *Macromolecules* **1990**, *23*, 4769.
(21) Shull, K. R. *J. Chem. Phys.* **1991**, *94*, 5723.
(22) Russell, T. P.; Hjelm, R. P.; Seeger, P. *Macromolecules* **1990**, *23*, 890.
(23) Olvera de la Cruz, M.; Sanchez, I. C. *Macromolecules* **1987**, *20*, 440.
(24) Hariharan, A.; Kumar, S. K.; Russell, T. P. *Macromolecules*, in press.